UC Irvine
UC Irvine Previously Published Works

Title
Glucose Transporter 1-Positive Endothelial Cells in Infantile Hemangioma Exhibit Features of Facultative Stem Cells

Permalink
https://escholarship.org/uc/item/1435726r

Journal
Stem Cells, 33(1)

ISSN
1066-5099

Authors
Huang, Lan
Nakayama, Hironao
Klagsbrun, Michael
et al.

Publication Date
2015

DOI
10.1002/stem.1841

Peer reviewed

eScholarship.org Powered by the California Digital Library
University of California

NIH Public Access
Author Manuscript
Stem Cells. Author manuscript; available in PMC 2016 January 01.

Published in final edited form as:
Stem Cells. 2015 January ; 33(1): 133–145. doi:10.1002/stem.1841.

Glucose transporter 1-positive endothelial cells in infantile hemangioma exhibit features of facultative stem cells

Lan Huang[1,3], **Hironao Nakayama**[1,3], **Michael Klagsbrun**[1,3,4], **John B. Mulliken**[2,3], and **Joyce Bischoff**[1,3,*]

[1]Vascular Biology Program and Department of Surgery, Harvard Medical School, Boston, MA 02115

[2]Department of Plastic and Oral Surgery, Boston Children's Hospital, Harvard Medical School, Boston, MA 02115

[3]Department of Surgery, Harvard Medical School, Boston, MA 02115

[4]Department of Pathology, Harvard Medical School, Boston, MA 02115

Abstract

Endothelial glucose transporter 1 (GLUT1) is a definitive and diagnostic marker for infantile hemangioma (IH), a vascular tumor of infancy. To date, GLUT1-positive endothelial cells in IH have not been quantified nor directly isolated and studied. We isolated GLUT1-positive and GLUT1-negative endothelial cells from IH specimens and characterized their proliferation, differentiation and response to propranolol, a first-line therapy for IH, and to rapamycin, an mTOR pathway inhibitor used to treat an increasingly wide array of proliferative disorders. Although freshly isolated GLUT1-positive cells, selected using anti-GLUT1 magnetic beads, expressed endothelial markers CD31, VE-Cadherin and VEGFR2, they converted to a mesenchymal phenotype after three weeks in culture. In contrast, GLUT1-negative endothelial cells exhibited a stable endothelial phenotype *in vitro*. GLUT1-selected cells were clonogenic when plated as single cells and could be induced to re-differentiate into endothelial cells, or into pericyte/smooth muscle cells or into adipocytes, indicating a stem cell-like phenotype. These data demonstrate that, although they appear and function in the tumor as bona fide endothelial cells, the GLUT1-positive endothelial cells display properties of facultative stem cells. Pretreatment with rapamycin for 4 days significantly slowed proliferation of GLUT1-selected cells, whereas propranolol pretreatment had no effect. These results reveal for the first time the facultative nature of GLUT1-positive endothelial cells in infantile hemangioma.

[*]To whom correspondence should be addressed: Vascular Biology Program Karp Family Research Building 12.212 Boston Children's Hospital Boston, MA 02115 Phone: 617-919-2192 joyce.bischoff@childrens.harvard.edu.

Disclosure of potential conflicts of interest None

Author contributions: L.H. designed and performed all experiments, interpreted data, and drafted the manuscript. H.N. conducted western blots. M.K. provided expert advice in molecular assays. J.B.M. provided clinical expertise on IH, was involved in discussion of the project, and reviewed the manuscript. J.B. supervised the whole project, discussed experimental design, interpreted data, and drafted the manuscript.

NIH-PA Author Manuscript
NIH-PA Author Manuscript
NIH-PA Author Manuscript

NIH-PA Author Manuscript

NIH-PA Author Manuscript

NIH-PA Author Manuscript

Keywords

facultative stem cells; infantile hemangioma; glucose transporter 1; endothelial cells

Introduction

Infantile hemangioma (IH) is a common vascular tumor with a unique lifecycle of rapid growth for 6-8 months during infancy, forming a mass of perfused blood vessels, followed by slow, spontaneous regression over 3-7 years [1, 2]. Glucose transporter I (GLUT1) is expressed along the endothelium of hemangioma in the proliferating and involuting phases. Immunohistochemical (IHC) staining for GLUT1 is used to distinguish IH from other vascular tumors and vascular malformations [3, 4]. To date, there is no evidence of a functional role for GLUT1 in either the onset or involution of IH.

To identify the cellular drivers of hemangioma-genesis, our laboratory isolated hemangioma endothelial cells (HemEC) [5-7], hemangioma pericytes (HemPericyte) [8] [9] and hemangioma stem cells (HemSC) [10] from IH specimens. HemSC are purified based on expression of the human stem/progenitor cell marker CD133. HemSC proliferate rapidly in culture, exhibit a mesenchymal phenotype, and can be induced to differentiate into endothelial cells, pericytes and adipocytes [9, 10]. When injected subcutaneously in immune-deficient mice, HemSC form GLUT1-positive ($GLUT1^+$) hemangioma-like blood vessels [10, 11]. After one month, a process akin to involution ensues as human blood vessels diminish and human adipocytes appear in the sub-cutaneous implants. Taken together, these findings show HemSC recapitulate the signature features of IH in this murine model.

While HemSC can form $GLUT1^+$ endothelium in mice, it has not been shown whether the $GLUT1^+$ endothelial cells, which are so prominent in IH histology, are descended from HemSC, nor has the hemangioma-forming potential of $GLUT1^+$ cells been tested. Therefore, we set out to specifically isolate and characterize $GLUT1^+$ endothelial cells to assess their functions in IH.

IHC staining and transcriptional profiling has shown that high levels of JAGGED1, angiopoietin-2 [12], E-selectin [13], and SKI oncogene [14] are expressed in IH endothelium in the proliferating phase. HemEC isolated from proliferating phase IH also express high levels of JAGGED1 [9], angiopoietin-2 [15], and E-selectin [7], consistent with the immunostaining and transcriptional profiling of endothelium from IH. Furthermore, HemEC *in vitro* exhibit an immature phenotype [6, 16], constitutively phosphorylated vascular endothelial growth factor receptor 2 (VEGFR2) and low expression of VEGFR1 [17] in comparison with human endothelial cells from newborn foreskin. Levels of GLUT1 in HemEC have not been reported.

Although benign, IH can threaten vital organs and tissues, ulcerate, and leave the child with significant structural abnormalities or disfigurement after the tumor involutes. We showed that corticosteroid, a long-established treatment for problematic IH, suppresses VEGF-A expression in HemSC and inhibits the ability of HemSC to form hemangioma-like vessels in

NIH-PA Author Manuscript

NIH-PA Author Manuscript

NIH-PA Author Manuscript

mice [18]. Propranolol, a nonselective β-adrenergic receptor blocker, is a new treatment that has rapidly become first-line therapy for IH [19-22]. At present, there is little information regarding the mechanism(s) by which the drug slows or halts the growth of IH or in regard to the rebound that occurs in some cases when propranolol therapy is stopped [23, 24]. We demonstrated that 4 day pre-treatment of HemSC with rapamycin, an mTOR inhibitor, blocked their vessel-forming ability *in vivo* and reduced their clonogenic and proliferative capacity *in vitro* [25]. Furthermore, rapamycin has shown some efficacy in a child with severe IH who failed other therapies [26]. Despite advances in treatments for children with IH, there is still a pressing need for improved strategies, perhaps involving combinations of drugs, to prevent IH from reaching an endangering size and to shorten the duration of drug therapy during infancy.

In this study, we show that $GLUT1^+$ endothelial cells are significantly decreased in IH specimens from children over one year of age, i.e. tumors that have entered the involuting phase. We also demonstrate stem cell-like properties of $GLUT1^+$ endothelial cells that become evident when these cells are removed from the tumor, purified and expanded *in vitro*. Finally, we show that a 4 day pre-treatment with rapamycin suppresses the proliferative potential of the GLUT1-selected cells, whereas propranolol pre-treatment does not. Conversion of $GLUT1^+$ endothelial cells in IH to stem-like cells reveals for the first time their “facultative” nature, i.e., the potential to adopt alternative phenotypes when the microenvironment is altered.

Materials and Methods

Cell isolation and culture

IH specimens (n=17, see Table 1) were obtained under a human subject protocol approved by the Committee on Clinical Investigation at Boston Children’s Hospital. Informed consent was obtained, according to the Declaration of Helsinki. The clinical diagnosis was confirmed by histopathology. Single cell suspensions were prepared by digesting IH specimens with Liberase^{TM} (Roche, Indianapolis, IN). $GLUT1^+$ endothelial cells were selected (n=5, Hem158, 159, 161,162 and 163) using mouse anti-human GLUT1 antibody (R&D Systems, Minneapolis, MN) followed by anti-mouse IgG Dynabeads (Life Technologies, Grand Island, NY). Because all $GLUT1^+$ cells are endothelial cells in proliferating hemangioma (Figure 1C), anti-GLUT1 selection is an efficient means to capture $GLUT1^+$ endothelial cells. GLUT1-negative ($GLUT1^{neg}$) cells were selected using anti-human CD31 Dynabeads (Life Technologies) to yield $GLUT1^{neg}CD31^+$ cells. A schematic of the isolation procedure is shown in Figure 2A. The freshly isolated cells were either directly lysed for RNA isolation or plated on fibronectin (1 μg/cm^2, EMD Millipore, Billerica, MA)-coated plates in Endothelial Growth Medium-2 (EGM-2), which includes Endothelial Basal Medium (EBM2, Lonza, Allendale, NJ) supplemented with 10% FBS, Endothelial Growth Media-2 SingleQuots (Lonza), and 1X GPS (Mediatech Inc, Manassas,VA, 100 U/milliliter (mL) penicillin, 100 μg/mL streptomycin, 292 μg/mL Glutamine) and cultured at 37°C in a humidified incubator with 5% CO_2. Ten days after plating, $GLUT1^+$ cells were selected with anti-human CD31 Dynabeads to yield $GLUT1^+CD31^+$ cells. Hereafter, the double-selected $GLUT1^+CD31^+$ cells are called

NIH-PA Author Manuscript

NIH-PA Author Manuscript

NIH-PA Author Manuscript

GLUT1-selected ($GLUT1^{sel}$) cells. At this time, $GLUT1^{neg}CD31^{+}$ cells were subjected to a second round of anti-CD31-selection to further enrich for endothelial cells.

Human umbilical cord blood was obtained from healthy newborns (38-40 weeks gestational age) from the Brigham and Women's Hospital under an IRB-approved protocol. Endothelial colony forming cells (ECFCs) were isolated from cord blood as described [27, 28]. Hemangioma-derived stem cells (HemSC) and adult human bone marrow mesenchymal stem were isolated and maintained in our laboratory as described [10].

Single cell clonogenic assay

Early passage (p2-p3) $GLUT1^{sel}$ and $GLUT1^{neg}CD31^{+}$ cells were plated at one cell per well into 96 well plates pre-coated with fibronectin in 200 μl of EGM-2 medium and cultured at 37°C [29]. Media was changed every five days. After 14 days, cells were fixed with 4% paraformaldehyde (Sigma; St. Louis, MO) for 30 minutes at room temperature, washed twice, stained with 1.5 μg/ml DAPI, and examined for colonies under a fluorescent microscope through a 10x objective lens. Wells containing two or more cells were identified as positive for proliferation. Wells containing fewer than 50 cells were counted by visual inspection with a fluorescent microscope through a 40x objective lens. For those wells with more than 50 cells, colonies were imaged and cell number quantified using an Image J1.38v program (Wayne Rasband, NIH).

Endothelial, pericytic and adipogenic differentiation assays

To induce endothelial differentiation, $GLUT1^{sel}$ cells were cultured for 5 days in serum-free EBM-2 medium containing 1x insulin-transferrin-selenium, 1x linoleic-acid albumin, 100μM ascorbic acid 2-phosphate, 1 μM dexamethasone. The same media with 10ng/mL epidermal growth factor (EGF) and 10ng/mL platelet-derived growth factor (PDGF)-BB served as a control, maintaining cells in serum free media without differentiation, as shown previously for HemSC and human multipotent adult progenitor cells [10, 30].

For pericytic/smooth muscle cell differentiation, $GLUT1^{sel}$ cells were co-cultured with ECFCs as ratio1:1 for 5 days in EGM-2 media [9]. Thereafter, $GLUT1^{sel}$ cells were separated from ECFCs using anti-human CD31 Dynabeads.

For adipogenesis, $GLUT1^{sel}$ cells were cultured in adipogenic media (DMEM, 10%FBS, 5μg/mL insulin, 1 μM dexamethasone, 0.5 mM isobutylmethylxanthine, 60 μM indomethacin, and 1x GPS) for 10 days. Lipid droplets were detected with Oil-Red-O staining. Images were acquired with a Nikon Eclipse TE 300 (Nikon, Melville, NY) using Spot advance v3.5.9 software (Diagnostic Instruments, Sterling Heights, MI).

Flow cytometry

Freshly isolated or cultured cells (1×10^5) were incubated at 4°C for 30 minutes in 100 μl of PBS plus 1% bovine serum albumin (BSA) with the primary antibody, washed three times, and analyzed by flow cytometry (Becton Dickinson, San Diego, CA). Primary antibodies were anti-human CD45 conjugated to allophycocyanin (APC) (eBioscience; San Diego, CA), anti-human Glycophorin A conjugated to APC (eBioscience), anti-human CD31

NIH-PA Author Manuscript

NIH-PA Author Manuscript

NIH-PA Author Manuscript

conjugated to phycoerythrin (PE) (BD Biosciences Pharmingen; Bedford, MA), anti-human CD34 conjugated to PE (Miltenyi Biotec; Auburn, CA), anti-human VECadherin (VECad/CD144) conjugated to PE (R&D Systems), anti-human vascular endothelial growth factor receptor2 (VEGFR2) conjugated to PE (R&D Systems), anti-human GLUT1 conjugated to fluorescein isothiocyanate (FITC) (R&D Systems), anti-human CD90 conjugated to PE (R&D Systems), anti-human Platelet-derived growth factor receptor β (PDGFRβ) conjugated to FITC (R&D Systems), anti-human NG2 conjugated to FITC (R&D Systems), and anti-human alpha-smooth muscle actin (αSMA) conjugated to PE (R&D Systems). For negative controls, we used fluorescently conjugated mouse isotype-matched control IgG (R&D Systems). Data was analyzed using Flowjo_10v software (Tree Star, Inc. Ashland, OR).

RNA isolation and quantitative reverse transcriptase PCR (QPCR)

Total cellular RNA was extracted with an RNeasy Micro extraction kit (Qiagen, Valencia, CA). Reverse transcriptase reactions were performed using an Omniscript RT Kit (Qiagen). QPCR was performed using FastStart Universal SYBR Green Master 2x (Rox) (Roche). Amplification was carried out in an ABI 7500 (Applied Biosystems, Foster City, CA). A standard curve for each gene was generated to determine amplification efficiency and relative expression. ECFC were used to generate standard curves for endothelial markers, hemangioma pericyes were used to generate the standard curve for PDGFRβ and GLUT1^{sel} cells were used to generate the standard curve for GLUT1. ATP5B and HPRTI were used as housekeeping gene expression references. Quantitative analysis was performed according to Pfaffl's method [31]. Primer sequences are shown in Supplemental Table 1.

Western blots

Cell extracts were prepared [9, 32], electrophoresed by sodium dodecyl sulfate–polyacrylamide gel electrophoresis (SDS-PAGE), transferred to nitrocellulose, and probed with anti-human PlexinD (R&D Systems), anti- αTubulin (EMD Millipore), anti-JAGGED1(Cell Signaling Technology, Danvers, MA), anti-human Calponin (Dako, Carpinteria, CA), anti-human CD31 (Santa Cruz Biotechnology, Inc., Dallas, Texas), anti-human sm22α (Abcam, Cambridge, MA) and anti-human β-actin (Abcam) antibodies. All signals detected by enhanced chemiluminescence.

Implantation of hemangioma-derived cells into nu/nu mice

GLUT1^{sel} cells or HemSCs were trypsizined, counted, and suspended in Phenol Red-free Matrigel (BD Biosciences) [10, 18]. Cell/Matrigel mixtures (4×10^6 cells/250 μL) were injected subcutaneously into flanks of anesthetized 6 to 9-week male nu/nu mice (Massachusetts General Hospital, Boston MA). After 14 days, mice were euthanized and implants excised and analyzed by histology and immunohistochemistry (N=5).

Histology and immunohistochemistry

Formalin-fixed, paraffin-embedded tissue sections (5μm) were deparaffinized and either directly stained with hematoxylin and eosin (H&E) or immersed in a antigen retrieval solution (either Citrate-EDTA buffer: 10mM Citric Acid, 2mM EDTA, 0.05% Tween-20,

NIH-PA Author Manuscript

NIH-PA Author Manuscript

NIH-PA Author Manuscript

pH 6.2; or Tris-EDTA buffer: 10mM Trizma Base, 1mM EDTA, 0.05% Tween-20, pH 9.0; or 20 ug/mL proteinase K) for 20 minutes. Sections were blocked for 30 minutes in 5% serum and stained with anti–human CD31 (clone JC70A, Dako), anti-human GLUT1 (Clone SPM498, Abcam), anti-human Calponin1 (Sigma), anti-human Perilipin A (Sigma), anti-human nuclear antigen (Clone 5H2, Chemicon), anti-human ERG1 (Santa Cruz Biotechnology), anti-human Vimentin (Clone V9, Abcam) and anti-mouse CD31 (Clone MEC13.3, BD Biosciences Pharmingen). Purified class- and species-matched IgGs (Vector Lab) were used as controls. For immunohistochemistry, sections were incubated with appropriate biotinylated secondary antibodies (Vector Lab) and streptavidin-horseradish peroxidase (HRP) (Vector lab), followed by 3,3-diaminobenzidine (DAB) (Vector lab). Slides were mounted using hematoxylin as nuclear marker and analyzed through a 40x objective lens in Zeiss Axio Imager M1 microscope (Carl Zeiss Microscopy, LLC). For immuno-fluorescent staining, sections were incubated with the appropriate FITC or Texas Red conjugated secondary antibody (Vector Lab). Tyramide Signal Amplification (TSA) Kit (PerkinElmer Inc., Waltham, MA) was applied in anti-mouse CD31 staining. All the slides were mounted using DAPI (Molecular Probe, Eugene, OR) as a nuclear marker. Images were acquired using a Leica TCS sp2 Acousto-Optical Beam Splitter confocal system equipped with DMIRE2 inverted microscope camera (Leica Microsystems, Wetzlar, Germany).

Rapamycin and Propranolol treatment

To test the longevity of anti-proliferative effects, a pre-treatment and then wash-out experiment was conducted. Cells at passages 4-5 were plated on FN-coated plates at 10,000 cells per cm^2. 16 hours later, media was removed and fresh EGM2 media with rapamycin (LC Laboratories, Woburn MA; 20ng/ml, equal to 22nM,) or the same volume of DMSO, propranolol (Sigma; 10μM) or the same volume of vehicle (sterile water, pH 3.0, prepared by the Boston Children's Hospital Pharmacy to match the solution in which propranolol was supplied) was added. Drug concentrations were chosen based on previous studies that showed anti-proliferative effects on hemangioma-derived cells [25, 33, 34]. Rapamycin was added every 2 days and propranolol was added twice a day. After 4 days, cells were washed with PBS 3 times, trypsinized and replated in a 48-well FN-coated plates at 10,000 cells per cm^2 in EGM2 media without drugs. Cells were counted after 6, 24, 48, 72 and 96 hours. Cells from Hem158, 159 and 163 were assayed.

Statistical analysis

Results are expressed as mean± the standard error of the mean (SEM) for the study variables. Comparison of the percent of $GLUT1^+$ EC in freshly isolated IH specimens was assessed by unpaired t test using GraphPad Prism version 5.00 (GraphPad Software, La Jolla, CA). Gene expression levels in $GLUT1^{sel}$ cells and $GLUT1^{neg}CD31^+$ cells were analyzed by paired t test; the same method was used for clonogenic assays. Change of gene expression after multi-lineage differentiation was assessed by ANOVA followed by paired Students t test when appropriate. The same method was applied to assessment of drug pre-treatment in proliferation assays. The MVD was evaluated by ANOVA. Significant differences were set at the $P<0.05$ level.

NIH-PA Author Manuscript

NIH-PA Author Manuscript

NIH-PA Author Manuscript

Results

GLUT1^{+} endothelial cells are decreased in involuting phase specimens of IH

GLUT1^{+} endothelial-lined blood vessels are a hallmark of IH in the proliferating and involuting phases [3, 4]. However, double-staining with antibodies against GLUT1 and the endothelial marker CD31 showed that GLUT1^{+}CD31^{+} and GLUT1-negative (GLUT1^{neg}) CD31^{+} vessels are present in the tumor (Figure 1A and Supplemental Figure 1). We used flow cytometry to quantify freshly isolated GLUT1^{+}EC versus GLUT1^{neg} EC in IH (Figure 1B-D). Hematopoietic cell populations were detected and gated out using anti-human CD45 and anti-human Glycophorin A (GlyA) antibodies (Figure 1B). Endothelial cells were labeled with a panel of PE-conjugated antibodies against the endothelial markers CD31, CD34, VE-Cadherin, and VEGFR2 to ensure all endothelial cells were detected. Cells were also simultaneously incubated with anti-GLUT1-FITC (Figure 1C,D). Cells were not permeabilized, so that antibody binding required cell surface localized antigens. This multi-antibody analysis demonstrated the presence of GLUT1^{+} EC and GLUT1^{neg} EC in IH and provided a means to quantify the relative proportions of the two populations in IH specimens removed from children ages 3 months to 7 years (n=15). The percentage of GLUT1^{+} EC was significantly increased in IH from patients less than one year of age compared to those over one year of age (Figure 1E).

GLUT1-selected (GLUT1^{sel}) cells convert to a mesenchymal phenotype *in vitro*

GLUT1^{+} EC and GLUT1^{neg} EC were isolated from proliferating hemangioma by antibody-conjugated magnetic beads (Day 0) (Figure 2A). Quantitative reverse transcriptase PCR (QPCR) performed immediately after the antibody-magnetic bead selection showed that GLUT1^{+} and GLUT1^{neg}CD31^{+} cells expressed endothelial markers CD31, VE-Cadherin, VEGFR2, and PlexinD1 [35, 36] but not the pericyte marker PDGFRβ (Supplemental Figure 2A). After 10 days expansion in culture, GLUT1^{+} cells were selected with anti-CD31 antibody-coated magnetic beads to yield GLUT1^{+}CD31^{+} cells. Hereafter, these double-selected, GLUT1^{+}CD31^{+} cells are designated GLUT1-selected (GLUT1^{sel}) cells. Again, QPCR was performed to verify cell purity (Supplemental Figure 2B).

After 3 weeks of culture, GLUT1^{sel} cells displayed a mesenchymal morphology that was distinctly different from GLUT1^{neg}CD31^{+} cells but similar to HemSC (Figure 2B). Flow cytometry (Figure 2C) revealed that GLUT1^{sel} cells no longer expressed endothelial markers CD31 and VEGFR2 but expressed the mesenchymal marker CD90, PDGFRβ and NG2. In contrast, GLUT1^{neg}CD31^{+} cells expressed endothelial markers but not CD90, PDGFRβ or NG2. Neither cell population expressed CD45, a common leukocyte cell marker. The cells were further analyzed by QPCR (Figure 2D). The GLUT1^{neg}CD31^{+} cells expressed all of the endothelial markers tested: CD31, VECadherin, JAGGED1, Angiopoietin-2, VEGFR2, PlexinD1, but only low levels of GLUT1 and VEGF-A. In contrast, GLUT1^{sel} cells lacked endothelial markers but expressed GLUT1 and VEGF-A. Of note, GLUT1 levels were reduced compared to the freshly isolated GLUT1^{+} cells, as were CD31 levels (Figure 2E and Supplemental Figure 2A). Down-regulation of GLUT1 in cultured cells is known [37]. GLUT1 protein expression was detected by flow cytometry in saponin-permeabilized cells, indicating an intracellular localization (Supplemental Figure 3). In summary, our results

NIH-PA Author Manuscript

NIH-PA Author Manuscript

NIH-PA Author Manuscript

indicate that after three weeks of *in vitro* expansion, GLUT1^{sel} cells down-regulated EC markers and converted to a mesenchymal phenotype, while the GLUT1^{neg}CD31^{+} cells remained endothelial.

GLUT1^{sel} cells display vascular progenitor properties *in vitro*

The proliferative ability of GLUT1^{sel} cells was assessed in a single-cell clonogenic assay (Figure 3A). Fourteen days after plating one cell per well, the number of wells with dividing cells and number of cells in each colony was determined. The percent single cells undergoing division was similar between GLUT1^{sel} cells and GLUT1^{neg}CD31^{+} cells (71.6 ± 1.3 vs. 51.5 ± 5.8, respectively). Of the GLUT1^{sel} cells that divided, 40.0 ± 9.0% gave rise to well-circumscribed colonies containing more than 10,000 cells. This was significantly higher than GLUT1^{neg}CD31^{+} cells (0.8 ± 0.8%, $p<0.0001$). In contrast, the majority of dividing GLUT1^{neg}CD31^{+} cells (28.0 ± 8.0%) formed small sized colonies (fewer than 50 cells) while only 13.2 ± 3.1% of plated GLUT1^{sel} cells formed small sized colonies. Thus, GLUT1^{sel} cells displayed a robust clonogenic capacity, a property shared with many types of stem and progenitor cells, including HemSC [25].

We next examined whether GLUT1^{sel} cells could be induced to undergo endothelial, pericytic and adipogenic differentiation, as has been shown for HemSC [9, 10, 32]. When cultured in EC differentiation media for 5 days, endothelial markers VE-Cadherin (Figure 3B), PlexinD1 and JAGGED1 (Figure 3C) were increased in GLUT1^{sel} cells, compared to the control conditions of EGM2 media or EC differentiation media with PDGF-BB and EGF. QPCR showed that PlexinD1 and JAGGED1 mRNAs were also upregulated (Figure 3D). CD31 mRNA showed a trend towards increased expression in GLUT1^{sel} cells induced to undergo endothelial differentiation. Immunofluorescence staining showed modest but evident expression of ERG1, an important endothelial transcriptional factor, in GLUT1^{sel} cells during EC differentiation (Figure 3E). Thus, endothelial cell markers can be re-induced in cultured GLUT1^{sel} cells *in vitro*.

We next examined whether GLUT1^{sel} cells can differentiate to a pericytic /SMC phenotype when co-cultured with normal human endothelial colony forming cells (ECFC) (Figure 4A). After 5 days of co-culture, the pericyte/SMC markers αSMA (Figure 4B), calponin and sm22α were induced in GLUT1^{sel} cells (Figure 4C). Such induction was confirmed in GLUT1^{sel} cells that were separated from ECFCs after the co-culture, using anti-CD31-coated magnetic beads (Figure 4C). The increases in protein expression were confirmed at the mRNA level (Figure 4D). Therefore, GLUT1^{sel} cells, like HemSC (Supplemental Figure 4), can be induced to express pericyte/SMC markers αSMA, calponin, sm22α, PDGFRβ and NG2.

GLUT1^{sel} cells also exhibited adipogenesis when cultured in adipogenic differentiation medium, as indicated by formation of lipid droplets, detected with Oil-Red-O (Figure 4E). HemSC and human bone marrow mesenchymal stem cells were analyzed in parallel as positive controls. GLUT1^{neg}CD31^{+} cells and ECFCs showed no indication of lipid droplets or positive Oil-Red-O staining. In summary, these experiments show that *in vitro* cultured GLUT1^{sel} cells are highly clonogenic and capable of endothelial, pericytic, and adipogenic differentiation, properties shared with HemSC.

NIH-PA Author Manuscript

NIH-PA Author Manuscript

NIH-PA Author Manuscript

GLUT1^{sel} cells undergo endothelial, pericytic and adipogenic differentiation in vivo

We next investigated the differentiative capacity of GLUT1^{sel} cells in a murine model of vasculogenesis. GLUT1^{sel} cells from three different IH were suspended in Matrigel and injected subcutaneously into nude mice. Fourteen days later, implants were harvested, sectioned, and stained with H&E, which revealed the presence microvessels perfused with red blood cells (Figure 5A). Quantification (Figure 5A, graph) showed that vessel formation was similar among GLUT1^{sel} cells from three different IH and to HemSCs described previously [10].

To assess whether the vessels were human or murine, antibodies specific for human CD31 and mouse CD31 were used to stain the sections (Figure 5B i and iii). Most vessels were negative for human CD31 but stained positive for mouse CD31. Clusters of human CD31^{+} cells within the implants were detected, but these were not organized into recognizable blood vessels. Nevertheless, these disorganized cells resembled some clusters of endothelial cells seen in proliferating IH (Figure 5B ii). Quantification of human CD31^{+} cells is shown in Figure 5B, graph. Adjacent sections were also stained with an anti-human calponin (Figure 5C i — iii) or anti-human vimentin (Figure 5C iiii — vi) antibodies to detect pericyte/smooth muscle cells [38]. Human calponin^{+} and vimentin^{+} cells appeared to be abluminal to the murine CD31^{+} blood vessels, which indicated that the human GLUT1^{sel} cells differentiated into perivascular cells in this model.

Adipocytes were detected in sections of the Matrigel implants after 14 days by staining with anti-perilipin A to highlight lipid storage droplets (Figure 5D). An anti-human nuclear antigen antibody was used to determine if the adipocytes were murine or differentiated from human GLUT1^{sel} cells. Some adipocytes stained positive for the human nuclear antigen (Figure 5D, black arrows), suggesting they had arisen from GLUT1^{sel} cells, whereas some cells were negative (*, Figure 5D) suggesting that either murine adipocytes were recruited into the Matrigel or murine mesenchymal cells were recruited and differentiated into adipocytes. In summary, these IHC studies indicate that GLUT1^{sel} cells can differentiate into ECs in Matrigel implants, but at 14 days had not formed functional endothelium. At 14 days, the GLUT1^{sel} cells can also differentiate into perivascular cells, which surround murine endothelium, and into adipocytes.

Pre-treatment with rapamycin suppresses proliferation of GLUT1^{sel} cells

Rapamycin diminishes the self-renewal and vasculogenic ability of HemSC [25]. However, HemSC constitute only 0.2-2% of the cells in proliferating IH [10, 39] and there is no direct evidence that HemSC actively proliferate *in vivo*. EC are the major, proliferative cell population in IH [12, 13, 40] and over 25% of them are GLUT1^{+} (Figure 1B-D). We examined the effect of a limited, 4 day pretreatment with rapamycin on the subsequent proliferation of GLUT1^{sel} and GLUT1^{neg}CD31^{+} cells over a subsequent 4 days in culture (Figure 6A). Rapamycin dramatically reduced the proliferation of GLUT1^{sel} cells (Figure 6B) whereas the same pretreatment with propranolol had no effect (Figure 6C). Rapamycin pretreatment also suppressed the more slowly proliferating GLUT1^{neg}CD31^{+} (Figure 6B) cells while propranolol had little effect (Figure 6C). These experiments demonstrate that the proliferative capacity of GLUT1^{sel} cells is significantly reduced after limited exposure to

NIH-PA Author Manuscript

NIH-PA Author Manuscript

NIH-PA Author Manuscript

rapamycin. In contrast, propranolol, added to the cells every 12 hours over the 4 day pre-treatment window, did not alter the proliferation of GLUT1^{sel} cells during a subsequent "drug-free" 4 day proliferation assay.

Discussion

Our study is the first to show that GLUT1^{+} endothelial cells in IH express properties of facultative stem cells. The GLUT1^{+} EC exhibit phenotypic and functional characteristics of endothelium, but when removed from the tumor environment and placed in culture as a purified population, they express stem cell-like properties of clonogenicity and multi-lineage differentiation.

Our study uncovered additional, novel findings. We show that the percentage of EC expressing GLUT1 on the cell surface is decreased in the involuting phase of IH. We optimized the endothelial quantification by using panel of antibodies against endothelial markers (CD31, CD34, VE-Cadherin and VEGFR2) to ensure all endothelial cells were captured. The decrease in GLUT1^{+} endothelium in the involuting phase, i.e. over one year of age, confirms the findings of a previous, non-quantitative study [41]. Sensitivity of GLUT1^{sel} cells to rapamycin is, potentially, a clinically important finding. A limited, 4 day pre-treatment of the GLUT1^{sel} cells with rapamycin was sufficient to block proliferation in a subsequent 4 day "drug-free" proliferation assay. In contrast, propranolol pre-treatment did not inhibit subsequent proliferation of either GLUT1^{sel} or GLUT1^{neg}CD31^{+} cells. We propose that rapamycin administration may prevent rapid proliferation of IH when used for limited treatment times or intervals. To pursue this concept, a clinical trial would be required to test whether pre-treatment with rapamycin or concurrent treatment with rapamycin and propranolol would more rapidly halt growth, accelerate involution and/or prevent rebound growth of IH.

Facultative stem cells are differentiated cells that harbor stem cell-like qualities. In response to a microenvironmental change, such as caused by stress or injury, these cells adopt a stem or progenitor-like phenotype to replenish cells as needed. Two examples are the facultative stem cells in adult liver and pancreas [42, 43] After exposure to hepatic-specific toxins, oval cells emerge that can give rise to biliary epithelial cells and hepatocytes, and thereby effectively contribute to hepatic regeneration [42]. Acinar cells in the adult pancreas can switch identity after pancreatic duct ligation and display features of multipotent progenitors that can generate ductal and endocrine cells. Emerging evidence supports the concept that facultative stem cells play important roles in organ/tissue repair and regeneration. The presence of and potential roles of facultative stem cells in vascular tumors, vascular anomalies or in settings of vascular regeneration has not heretofore been reported in the literature.

In the current study, we demonstrate that GLUT1^{sel} cells are a facultative stem cell population: in vivo they are phenotypically and functionally bona fide endothelial cells but when removed from the tumor and placed *in vitro* (a stress) they exhibit stem cell-like properties. They are clearly distinct from the GLUT1^{neg}CD31^{+} cells that display a stable endothelial phenotype in culture. We, and others, previously designated GLUT1^{neg}CD31^{+}

NIH-PA Author Manuscript

NIH-PA Author Manuscript

NIH-PA Author Manuscript

cells as HemEC. GLUT1^{sel} cells are similar but not identical to HemSC. GLUT1^{sel} cells did not form the endothelial lining of perfused blood vessels in the cell/Matrigel implant model; their endothelial re-differentiative capacity was limited to expression of endothelial markers. Whether GLUT1^{+} ECs in IH originate from HemSC or conversely GLUT1^{+} ECs undergo EC-to-HemSC transition is unknown and cannot be addressed by analysis of IH patient specimens. Our study does show that GLUT1^{+} ECs decrease during the involuting phase, indicating a quantitative loss of facultative stem cells as IH regresses.

Tumor endothelium and endothelium expressing constitutively active activin-like kinase-2 (ALK2) display a mesenchymal stem cell-like phenotype [44, 45], which may involve endothelial-to-mesenchymal transition (EndMT), a process known to occur during embryonic development [46, 47]. Therefore, we tested whether GLUT1^{neg}CD31^{+} cells could be induced to undergo EndMT, and thereby adopt a mesenchymal phenotype akin to the GLUT1^{sel} cells, by treating cells with recombinant TGFβ2 for 5 days (Supplemental Figure 5A) or TGFβ2 plus TNFα for 3 days (Supplemental Figure 5B). GLUT1^{neg}CD31^{+} cells did not consistently upregulate EndMT markers (αSMA and SNAI 2). Thus, it is unlikely that GLUT1^{neg}CD31^{+} cells undergo EndMT and contribute to the GLUT1^{sel} cell population. It was not possible to study EndMT in the GLUT1^{sel} cells because they acquired a mesenchymal phenotype by the time they were expanded sufficiently for such experiments.

GLUT1 is the most common glucose transporter in humans and is expressed in specific cell types, including erythrocytes, T-lymphocytes and endothelial cells located in the placenta and brain [48]. GLUT1 is an important diagnostic marker for IH, where it is prominently detected along the endothelium, but its possible functional significance in the pathogenesis of IH is unknown. Some investigators propose that presence of GLUT1 in IH may be a result of increased HIF1α that is perhaps stabilized due to hypoxia in an early stage of the tumor [49, 50]. Others suggest that GLUT1 is indicative of a placental origin of IH [4, 51]. We propose that GLUT1 marks facultative stem cells in the endothelium of IH.

We showed previously that rapamycin, an inhibitor of mTOR pathway, diminishes the self-renewal capacity of HemSC and that 4 day pretreatment in culture with rapamycin inhibits the ability of HemSC to form blood vessels in vivo [25]. Rapamycin can exert direct anti-angiogenic effects by inhibiting endothelial cell proliferation [52-54]. Here we tested the effect of rapamycin on the GLUT1-selected cell population because it is a major cellular component of IH. Four day pretreatment with rapamycin suppressed proliferation of GLUT1^{sel} cells in a subsequent 4 day “drug-free” proliferation assay. In contrast, pretreatment with propranolol did not inhibit subsequent proliferation (Figure 6). Concurrent treatment with propranolol has been shown to decrease the proliferation of hemangioma-derived EC to variable degrees [55-57], consistent with the clinical observation that propranolol must be present continuously to inhibit growth of IH. Our results suggest that a limited treatment with rapamycin might exert long anti-proliferative effects on the GLUT1^{+} EC in IH. We speculate that if used for a limited period of time, perhaps in combination propranolol or corticosteroid, rapamycin might enhance these treatments and shorten their duration.

NIH-PA Author Manuscript

NIH-PA Author Manuscript

NIH-PA Author Manuscript

Supplementary Material

Refer to Web version on PubMed Central for supplementary material.

Acknowledgments

We thank the Dana-Farber/Harvard Cancer Center for use of their Specialized Histopathology Core; Elisa Boscolo and David Smadja for helpful discussions; Lei Yuan for kindly providing ERG1 antibody for staining; Cassandra Rogers for acquiring microscopic images and Kristin Johnson for preparing figures.

Research reported in this manuscript was supported by the National Institute of Arthritis and Musculoskeletal and Skin Diseases, under Award Number P01 AR048564 (J.B.), and by the National Heart, Lung, and Blood Institute, under Award Number R01 HL 096384 (J.B.), both part of the National Institutes of Health. The content is solely the responsibility of the authors and does not necessarily represent the official views of the National Institutes of Health.

Funding: the National Institutes of Health, Grant Number P01 AR048564 (J.B.) and R01 HL096384 (J.B.)

References

1. Enjolras O, Mulliken JB. The current management of vascular birthmarks. Pediatr Dermatol. 1993; 10:311–313. [PubMed: 8302734]
2. Frieden IJ, Haggstrom AN, Drolet BA, et al. Infantile hemangiomas: current knowledge, future directions. Proceedings of a research workshop on infantile hemangiomas, April 7-9, 2005, Bethesda, Maryland, USA. Pediatr Dermatol. 2005; 22:383–406. [PubMed: 16190987]
3. North PE, Waner M, Mizeracki A, et al. GLUT1: a newly discovered immunohistochemical marker for juvenile hemangiomas. Hum Pathol. 2000; 31:11–22. [PubMed: 10665907]
4. North PE, Waner M, Mizeracki A, et al. A unique microvascular phenotype shared by juvenile hemangiomas and human placenta. Arch Dermatol. 2001; 137:559–570. [PubMed: 11346333]
5. Boye E, Yu Y, Paranya G, et al. Clonality and altered behavior of endothelial cells from hemangiomas. J Clin Invest. 2001; 107:745–752. [PubMed: 11254674]
6. Khan ZA, Melero-Martin JM, Wu X, et al. Endothelial progenitor cells from infantile hemangioma and umbilical cord blood display unique cellular responses to endostatin. Blood. 2006; 108:915–921. [PubMed: 16861344]
7. Smadja DM, Mulliken JB, Bischoff J. E-selectin mediates stem cell adhesion and formation of blood vessels in a murine model of infantile hemangioma. Am J Pathol. 2012; 181:2239–2247. [PubMed: 23041613]
8. Boscolo E, Mulliken JB, Bischoff J. Pericytes from infantile hemangioma display proangiogenic properties and dysregulated angiopoietin-1. Arterioscler Thromb Vasc Biol. 2013; 33:501–509. [PubMed: 23288163]
9. Boscolo E, Stewart CL, Greenberger S, et al. JAGGED1 signaling regulates hemangioma stem cell-to-pericyte/vascular smooth muscle cell differentiation. Arterioscler Thromb Vasc Biol. 2011; 31:2181–2192. [PubMed: 21757656]
10. Khan ZA, Boscolo E, Picard A, et al. Multipotential stem cells recapitulate human infantile hemangioma in immunodeficient mice. J Clin Invest. 2008; 118:2592–2599. [PubMed: 18535669]
11. Xu D, O TM, Shartava A, et al. Isolation, characterization, and in vitro propagation of infantile hemangioma stem cells and an in vivo mouse model. J Hematol Oncol. 2011; 4:54. [PubMed: 22192404]
12. Calicchio ML, Collins T, Kozakewich HP. Identification of signaling systems in proliferating and involuting phase infantile hemangiomas by genome-wide transcriptional profiling. Am J Pathol. 2009; 174:1638–1649. [PubMed: 19349369]
13. Kraling BM, Razon MJ, Boon LM, et al. E-selectin is present in proliferating endothelial cells in human hemangiomas. Am J Pathol. 1996; 148:1181–1191. [PubMed: 8644859]
14. O TM, Tan M, Tarango M, et al. Differential expression of SKI oncogene protein in hemangiomas. Otolaryngol Head Neck Surg. 2009; 141:213–218. [PubMed: 19643254]

NIH-PA Author Manuscript NIH-PA Author Manuscript NIH-PA Author Manuscript

15. Yu Y, Varughese J, Brown LF, et al. Increased Tie2 expression, enhanced response to angiopoietin-1, and dysregulated angiopoietin-2 expression in hemangioma-derived endothelial cells. Am J Pathol. 2001; 159:2271–2280. [PubMed: 11733376]
16. Dosanjh A, Chang J, Bresnick S, et al. In vitro characteristics of neonatal hemangioma endothelial cells: similarities and differences between normal neonatal and fetal endothelial cells. J Cutan Pathol. 2000; 27:441–450. [PubMed: 11028814]
17. Jinnin M, Medici D, Park L, et al. Suppressed NFAT-dependent VEGFR1 expression and constitutive VEGFR2 signaling in infantile hemangioma. Nat Med. 2008; 14:1236–1246. [PubMed: 18931684]
18. Greenberger S, Boscolo E, Adini I, et al. Corticosteroid suppression of VEGF-A in infantile hemangioma-derived stem cells. N Engl J Med. 2010; 362:1005–1013. [PubMed: 20237346]
19. Leaute-Labreze C, Dumas de la Roque E, Hubiche T, et al. Propranolol for severe hemangiomas of infancy. N Engl J Med. 2008; 358:2649–2651. [PubMed: 18550886]
20. Cheng JF, Gole GA, Sullivan TJ. Propranolol in the management of periorbital infantile haemangioma. Clin Experiment Ophthalmol. 2010; 38:547–553. [PubMed: 20553300]
21. Mazereeuw-Hautier J, Hoeger PH, Benlahrech S, et al. Efficacy of propranolol in hepatic infantile hemangiomas with diffuse neonatal hemangiomatosis. J Pediatr. 2010; 157:340–342. [PubMed: 20488455]
22. Rosbe KW, Suh KY, Meyer AK, et al. Propranolol in the management of airway infantile hemangiomas. Arch Otolaryngol Head Neck Surg. 2010; 136:658–665. [PubMed: 20644059]
23. Bagazgoitia L, Hernandez-Martin A, Torrelo A. Recurrence of infantile hemangiomas treated with propranolol. Pediatr Dermatol. 2011; 28:658–662. [PubMed: 22082463]
24. Marqueling AL, Oza V, Frieden IJ, et al. Propranolol and infantile hemangiomas four years later: a systematic review. Pediatr Dermatol. 2013; 30:182–191. [PubMed: 23405852]
25. Greenberger S, Yuan S, Walsh LA, et al. Rapamycin suppresses self-renewal and vasculogenic potential of stem cells isolated from infantile hemangioma. J Invest Dermatol. 2011; 131:2467–2476. [PubMed: 21938011]
26. Kaylani S, Theos AJ, Pressey JG. Treatment of Infantile Hemangiomas with Sirolimus in a Patient with PHACE Syndrome. Pediatr Dermatol. 2013
27. Ingram DA, Mead LE, Tanaka H, et al. Identification of a novel hierarchy of endothelial progenitor cells using human peripheral and umbilical cord blood. Blood. 2004; 104:2752–2760. [PubMed: 15226175]
28. Melero-Martin JM, De Obaldia ME, Kang SY, et al. Engineering robust and functional vascular networks in vivo with human adult and cord blood-derived progenitor cells. Circ Res. 2008; 103:194–202. [PubMed: 18556575]
29. Huang L, Critser PJ, Grimes BR, et al. Human umbilical cord blood plasma can replace fetal bovine serum for in vitro expansion of functional human endothelial colony-forming cells. Cytotherapy. 2011; 13:712–721. [PubMed: 21250867]
30. Reyes M, Dudek A, Jahagirdar B, et al. Origin of endothelial progenitors in human postnatal bone marrow. The Journal of clinical investigation. 2002; 109:337–346. [PubMed: 11827993]
31. Pfaffl MW. A new mathematical model for relative quantification in real-time RTPCR. Nucleic Acids Res. 2001; 29:e45. [PubMed: 11328886]
32. Boscolo E, Mulliken JB, Bischoff J. VEGFR-1 mediates endothelial differentiation and formation of blood vessels in a murine model of infantile hemangioma. Am J Pathol. 2011; 179:2266–2277. [PubMed: 21945324]
33. Medici D, Olsen BR. Rapamycin inhibits proliferation of hemangioma endothelial cells by reducing HIF-1-dependent expression of VEGF. PLoS One. 2012; 7:e42913. [PubMed: 22900063]
34. Lee D, Boscolo E, Durham JT, et al. Propranolol Targets Contractility of Infantile Hemangioma-derived Pericytes. The British journal of dermatology. 2014
35. Gu C, Yoshida Y, Livet J, et al. Semaphorin 3E and plexin-D1 control vascular pattern independently of neuropilins. Science. 2005; 307:265–268. [PubMed: 15550623]
36. Kim J, Oh WJ, Gaiano N, et al. Semaphorin 3E-Plexin-D1 signaling regulates VEGF function in developmental angiogenesis via a feedback mechanism. Genes Dev. 2011; 25:1399–1411. [PubMed: 21724832]

NIH-PA Author Manuscript NIH-PA Author Manuscript NIH-PA Author Manuscript

37. Tal M, Liang Y, Najafi H, et al. Expression and function of GLUT-1 and GLUT-2 glucose transporter isoforms in cells of cultured rat pancreatic islets. J Biol Chem. 1992; 267:17241–17247. [PubMed: 1512261]
38. Lin RZ, Moreno-Luna R, Li D, et al. Human endothelial colony-forming cells serve as trophic mediators for mesenchymal stem cell engraftment via paracrine signaling. Proceedings of the National Academy of Sciences of the United States of America. 2014; 111:10137–10142. [PubMed: 24982174]
39. Yu Y, Flint AF, Mulliken JB, et al. Endothelial progenitor cells in infantile hemangioma. Blood. 2004; 103:1373–1375. [PubMed: 14576053]
40. Mulliken JB, Glowacki J. Hemangiomas and vascular malformations in infants and children: a classification based on endothelial characteristics. Plast Reconstr Surg. 1982; 69:412–422. [PubMed: 7063565]
41. Yuan SM, Jiang HQ, Hong ZJ, et al. The expression and role of glucose transporter-1 in infantile hemangioma. Zhonghua Zheng Xing Wai Ke Za Zhi. 2007; 23:90–93. [PubMed: 17554865]
42. Yanger K, Stanger BZ. Facultative stem cells in liver and pancreas: fact and fancy. Dev Dyn. 2011; 240:521–529. [PubMed: 21312313]
43. Ziv O, Glaser B, Dor Y. The plastic pancreas. Dev Cell. 2013; 26:3–7. [PubMed: 23867225]
44. Dudley AC, Khan ZA, Shih SC, et al. Calcification of multipotent prostate tumor endothelium. Cancer Cell. 2008; 14:201–211. [PubMed: 18772110]
45. Medici D, Shore EM, Lounev VY, et al. Conversion of vascular endothelial cells into multipotent stem-like cells. Nat Med. 2010; 16:1400–1406. [PubMed: 21102460]
46. Tao G, Kotick JD, Lincoln J. Heart valve development, maintenance, and disease: the role of endothelial cells. Curr Top Dev Biol. 2012; 100:203–232. [PubMed: 22449845]
47. Kovacic JC, Mercader N, Torres M, et al. Epithelial-to-mesenchymal and endothelial-to-mesenchymal transition: from cardiovascular development to disease. Circulation. 2012; 125:1795–1808. [PubMed: 22492947]
48. Carruthers A, DeZutter J, Ganguly A, et al. Will the original glucose transporter isoform please stand up! Am J Physiol Endocrinol Metab. 2009; 297:E836–848. [PubMed: 19690067]
49. Kleinman ME, Greives MR, Churgin SS, et al. Hypoxia-induced mediators of stem/progenitor cell trafficking are increased in children with hemangioma. Arterioscler Thromb Vasc Biol. 2007; 27:2664–2670. [PubMed: 17872454]
50. Herbert A, Ng H, Jessup W, et al. Hypoxia regulates the production and activity of glucose transporter-1 and indoleamine 2,3-dioxygenase in monocyte-derived endothelial-like cells: possible relevance to infantile haemangioma pathogenesis. Br J Dermatol. 2011; 164:308–315. [PubMed: 21039406]
51. Barnes CM, Huang S, Kaipainen A, et al. Evidence by molecular profiling for a placental origin of infantile hemangioma. Proc Natl Acad Sci U S A. 2005; 102:19097–19102. [PubMed: 16365311]
52. Sehgal SN. Rapamune (RAPA, rapamycin, sirolimus): mechanism of action immunosuppressive effect results from blockade of signal transduction and inhibition of cell cycle progression. Clin Biochem. 1998; 31:335–340. [PubMed: 9721431]
53. Guba M, von Breitenbuch P, Steinbauer M, et al. Rapamycin inhibits primary and metastatic tumor growth by antiangiogenesis: involvement of vascular endothelial growth factor. Nat Med. 2002; 8:128–135. [PubMed: 11821896]
54. Phung TL, Ziv K, Dabydeen D, et al. Pathological angiogenesis is induced by sustained Akt signaling and inhibited by rapamycin. Cancer Cell. 2006; 10:159–170. [PubMed: 16904613]
55. Wong A, Hardy KL, Kitajewski AM, et al. Propranolol accelerates adipogenesis in hemangioma stem cells and causes apoptosis of hemangioma endothelial cells. Plast Reconstr Surg. 2012; 130:1012–1021. [PubMed: 23096601]
56. Stiles J, Amaya C, Pham R, et al. Propranolol treatment of infantile hemangioma endothelial cells: A molecular analysis. Exp Ther Med. 2012; 4:594–604. [PubMed: 23170111]
57. Ji Y, Li K, Xiao X, et al. Effects of propranolol on the proliferation and apoptosis of hemangioma-derived endothelial cells. J Pediatr Surg. 2012; 47:2216–2223. [PubMed: 23217879]

NIH-PA Author Manuscript

NIH-PA Author Manuscript

NIH-PA Author Manuscript

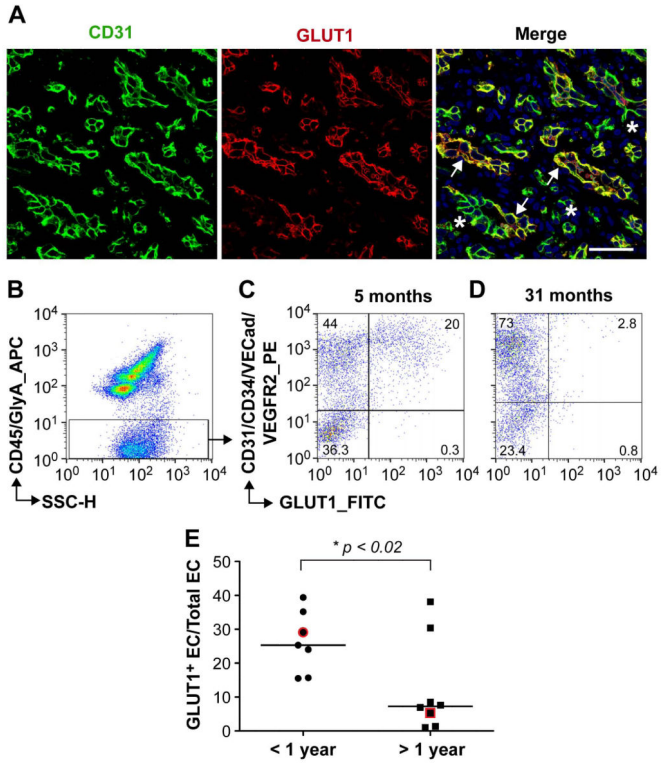

Figure 1. GLUT1^{+} and GLUT1^{neg} endothelial cells in IH

(A): Anti-human CD31 (green) and anti-GLUT1 (red) staining of proliferating IH tissue section (arrows, GLUT1^{+} vessels; *, GLUT1^{neg} vessels). Nuclei counterstained with DAPI (blue). Scale bar, 50 μm. Flow cytometric analyses of freshly isolated cells from proliferating IH (5 months old) (B-C) and involuting IH (31 months old) (D) using antibodies against human CD45/GlyA (APC), CD31/CD34/VECad/VEGFR2 (PE) and GLUT1 (FITC). Percentages of cells in each quadrant are shown (C,D). (E) Percent GLUT1^{+} ECs, quantified by flow cytometry, in IH specimens (N=15). •, IH specimens from children under one year of age; ■, IH specimens from children over one year of age. The specimens shown in C and D are highlighted in red. * p <0.02 by unpaired t test.

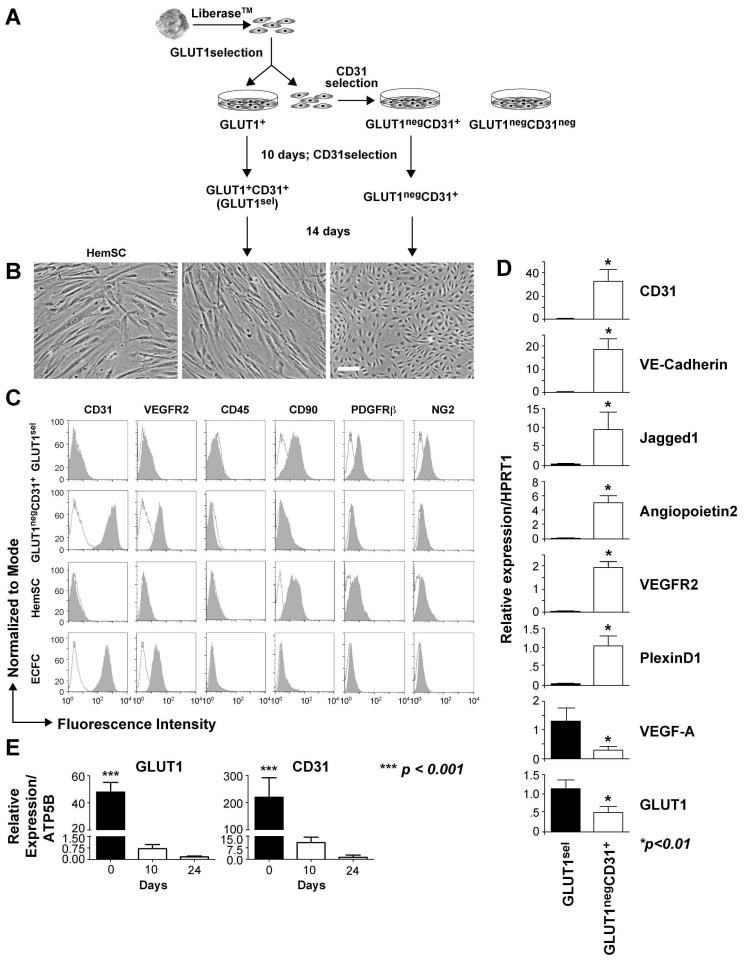

Figure 2. GLUT1^{sel} cells versus GLUT1^{neg}CD31^{+} cells

(A): Schematic of cell isolation using sequential antibody-coated magnetic beads. (B): Phase contrast image of GLUT1^{sel} cells and GLUT1^{neg}CD31^{+} cells after 3 weeks in culture. HemSC are shown for comparison on the left. Scale bar, 100 μm. (C): Flow cytometric analysis of GLUT1^{sel} cells and GLUT1^{neg}CD31^{+} cells for endothelial (CD31, VEGFR2), hematopoietic (CD45), and mesenchymal (CD90, PDGFRβ and NG2) markers. HemSC and ECFC included as controls. Black lines depict cells incubated with isotype-matched control antibodies; shaded grey areas are cells incubated with primary antibodies. (D): QPCR measured mRNA levels in GLUT1^{sel} cells (black bars) and GLUT1^{neg}CD31^{+} cells (white bars) after 3 weeks in culture (N=3). (E): QPCR measured mRNA levels of GLUT1 and CD31 in freshly anti-GLUT1 magnetic bead selected GLUT1^{+} cells on day0 and GLUT1^{sel} cells on day10 and 24 in the culture. * p <0.01 and *** p <0.0001 by paired t test.

NIH-PA Author Manuscript NIH-PA Author Manuscript NIH-PA Author Manuscript

NIH-PA Author Manuscript

NIH-PA Author Manuscript

NIH-PA Author Manuscript

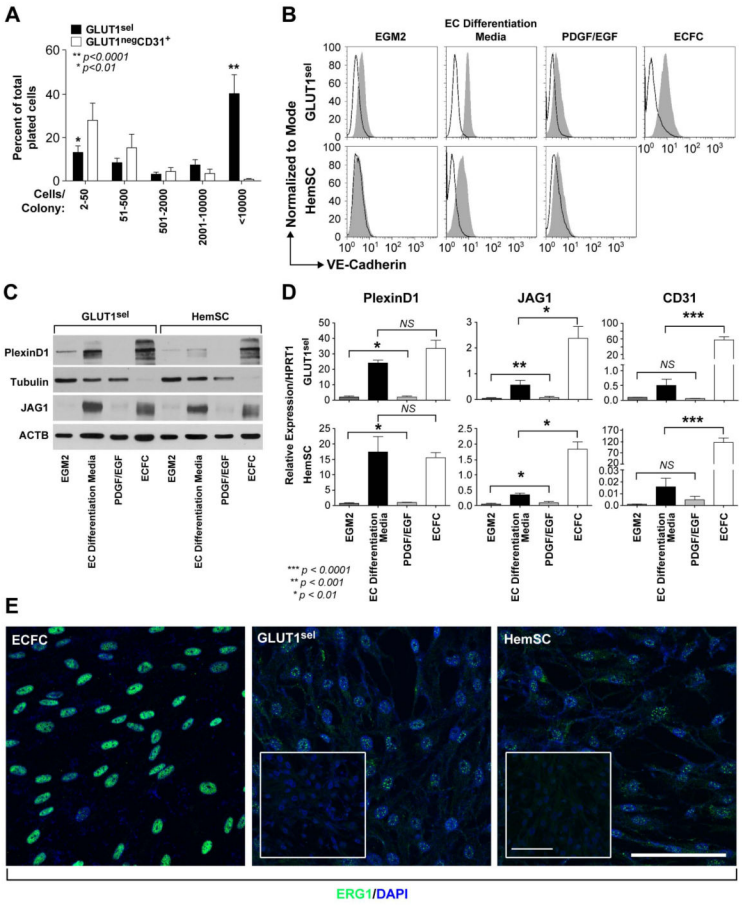

Figure 3. GLUT1^{sel} cells are clonogenic and can be induced to undergo endothelial differentiation *in vitro*

(A): GLUT1^{sel} cells (black bars) form larger colonies than GLUT1^{neg}CD31^{+} cells (white bars) in single cell clonogenic assays (N = 5). *P<0.01, **P<0.0001 by paired t test. (B-C): GLUT1^{sel} cells and HemSC induced to re-express endothelial markers after 5 days in EC differentiation media (N=4). Endothelial markers VE-Cadherin examined by flow cytometry (B) and PlexinD1 and Jagged1 (JAG1) examined by western blot (C). In B, black lines indicate cells incubated with isotype-matched control antibodies; shaded grey area, cells incubated with anti-VE-Cadherin antibody. ECFCs served as endothelial positive control in both. Cells cultured for 5 days in EGM-2 and in EC differentiation media with PDGF-BB and EGF served as negative controls. Tubulin or ACTB served as the loading control for the western blot. (D): QPCR for PlexinD1, Jagged1 (JAG1) and CD31 in GLUT1^{sel} cells and HemSC after 5 days of EC differentiation. ECFCs served as endothelial positive control. Cells cultured for 5 days in EGM-2 and in EC differentiation media with PDGFBB and EGF were negative controls. *P<0.01, **P<0.001 and ***P<0.0001 by ANOVA and unpaired t test. (E): Immunofluorescence staining for ERG1 in GLUT1^{sel} cells and HemSC after 5 days of EC differentiation. ECFC served as endothelial positive control. Insets are GLUT1^{sel} cells and HemSC that were not stimulated to undergo EC differentiation. Scale bar, 50 μm.

NIH-PA Author Manuscript

NIH-PA Author Manuscript

NIH-PA Author Manuscript

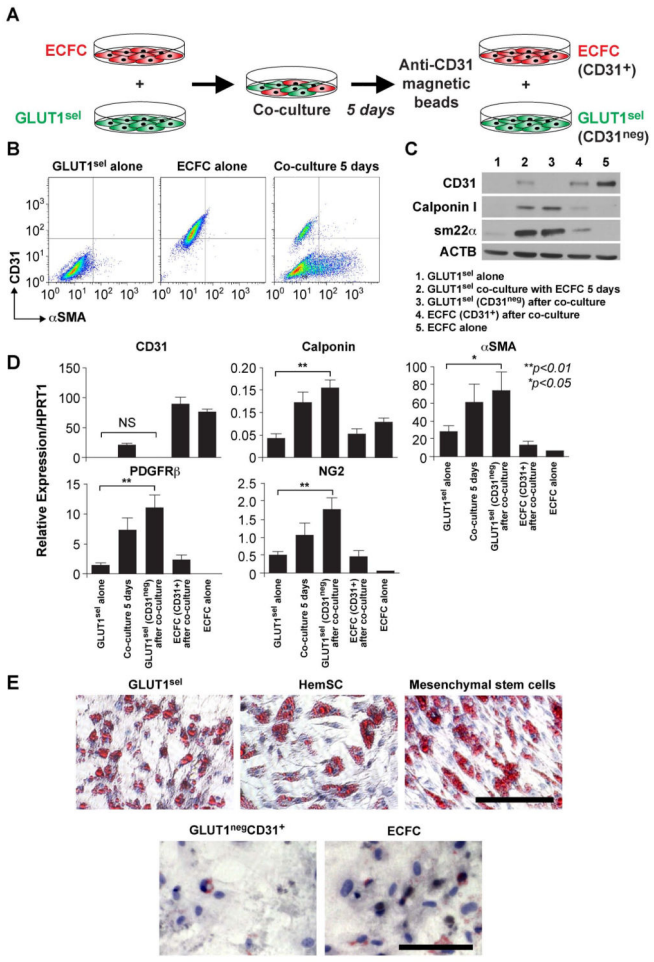

Figure 4. GLUT1^{sel} cells can be induced to express pericytic/SMC phenotype and undergo adipogenesis

(A): Schematic of pericyte/SMC differentiation assay: 5 days of co-culture with ECFCs, followed by removal with anti-CD31-coated magnetic beads. (B): CD31 and αSMA expression measured by flow cytometry of saponin-permeabilized cells. (C): Calpoinin I and sm22α measured by western blot. CD31 shown to evaluate ECFC removal. ACTB used as the loading control. (D): QPCR to analyze mRNA levels of pericyte/SMC markers. N=4, *P<0.05 and **P<0.01 by ANOVA followed by paired t test. (E): Cells induced to undergo adipogenesis stained with Oil Red-O. HemSC and mesenchymal stem cells served as positive controls; ECFC served as negative control. Scale bar, 80 μm. Results are representative of independent assays using paired GLUT1^{sel} and GLUT1^{neg}CD31^{+} cells isolated from 4 different IH specimens.

NIH-PA Author Manuscript

NIH-PA Author Manuscript

NIH-PA Author Manuscript

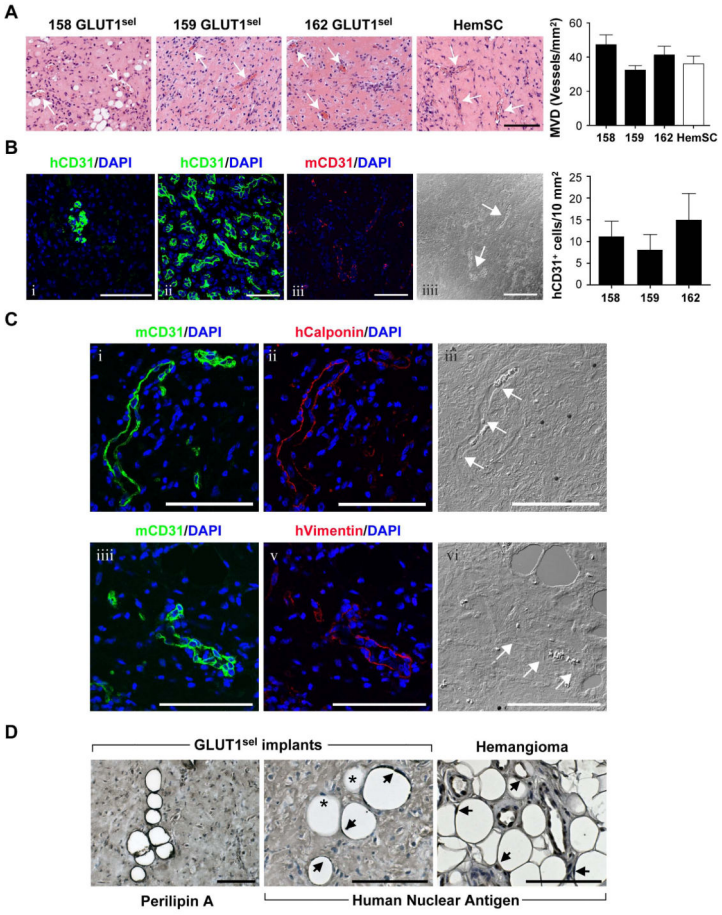

Figure 5. GLUT1^{sel} cells form ECs, pericytes/SMCs and adipocytes in immunodeficient mice

GLUT1^{sel} cells from 3 different IH (158,159 and 162) mixed with Matrigel and injected subcutaneously into nu/nu mice for 14 days. (A): H&E staining shows microvessels in the implants (white arrows indicate lumens with red blood cells). HemSC are shown for comparison. Scar bar, 150 μm. Microvessel density (MVD) quantified (N=5) and compared to HemSC [10]. (B): anti-human CD31 (green, i) staining of GLUT1^{sel} cell/Matrigel implants compared to anti-human CD31 staining of human IH specimen (green, ii). GLUT1^{sel} cell/Matrigel implant stained with anti-mouse CD31 (red, iii) with corresponding phase contrast image (iiii). White arrow indicates blood vessel lumen. Scale bar, 100 μm. Human CD31^{+} cells in the implants were quantified (N=5) (C): Serial sections from GLUT1^{sel} cell/Matrigel implant stained with anti-mouse CD31 (green, i) and anti-human Calponin (red, ii) with corresponding phase contrast image (iii). Serial sections from these implants stained with anti-mouse CD31 (green, iiii) and anti-human Vimentin (red, v), with corresponding phase contrast image (vi). White arrows indicate blood vessel lumen. Scale bar, 100 μm. (D): Anti-perilipin A staining of GLUT1^{sel} cell/Matrigel implants (left) panel and anti-human nuclear antigen staining of GLUT1^{sel} /Matrigel implants and involuting IH specimen (middle and right panels). Arrows indicate adipocytes stained with anti-human nuclei; * indicate non-stained adipocytes. Scale bar, 100 μm.

NIH-PA Author Manuscript

NIH-PA Author Manuscript

NIH-PA Author Manuscript

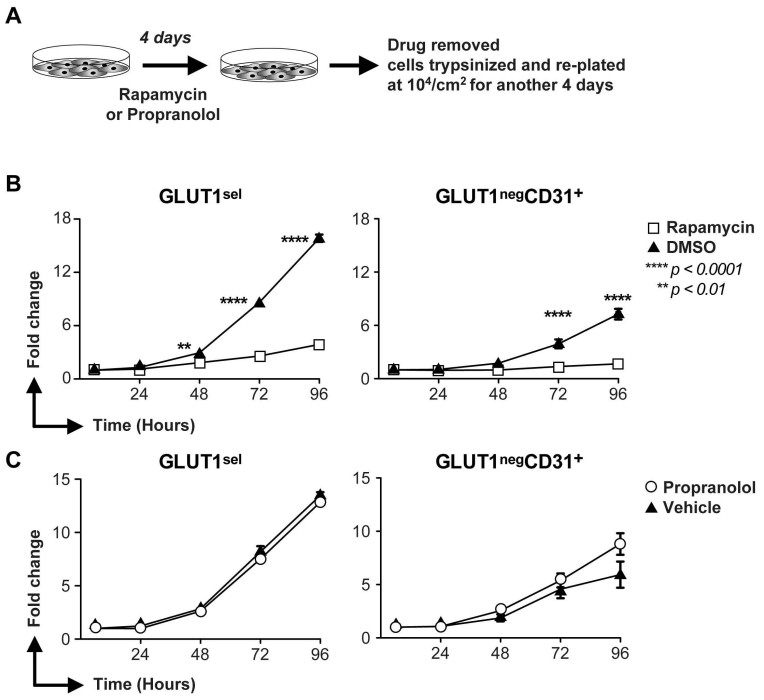

Figure 6. Rapamycin suppresses proliferation of GLUT1^{sel} cells and GLUT1^{neg}CD31^{+} cells *in vitro*

(A): Schematic of the experiment. (B): Proliferation of GLUT1^{sel} and GLUT^{neg}CD31^{+} cells in "drug-free" culture after 4-day pretreatment with rapamycin (B) or propranolol (C). Cells pretreated with DMSO (▲) in Panel B or vehicle (▲) in Panel C served as controls. N=3, **P<0.01 and ****P<0.0001 by ANOVA.

NIH-PA Author Manuscript
NIH-PA Author Manuscript
NIH-PA Author Manuscript

Table 1

Infantile Hemangioma Specimens

	Sample ID	Age	Gender
Proliferating (< 1 year)	Hem 154	3m	F
	Hem 162	3m	F
	Hem 157	4m	F
	Hem 153	5m	F
	Hem 156	6m	F
	Hem 161	8m	F
	Hem 159	8m	M
	Hem 163	9m	F
	Hem 158	12m	F
Involuting (> 1 year)	Hem I-75	1y5m	F
	Hem I-88	2y2m	F
	Hem I-86	2y6m	M
	Hem I-78	2y7m	M
	Hem I-87	2y10m	F
	Hem I-81	2y11m	F
	Hem ID-19	7y	F
	Hem ID-20	7y2m	F